

# Age of the Tananwan Formation in Northern Taiwan: A Reexamination of the Magnetostratigraphy and Calcareous Nannofossil Biostratigraphy

Chorng-Shern Horng\*

*Institute of Earth Sciences, Academia Sinica, Taipei, Taiwan, Republic of China*

Received 27 August 2013, accepted 5 November 2013

---

## ABSTRACT

Over the past two decades, the succession strata of the Tananwan Formation exposed horizontally on the Linkou Tableland in northwestern Taiwan has been either dated to a short time interval of 0.9 - 0.7 Ma or assigned to a vague long period within the Matuyama Epoch covering probably both the Olduvai and Jaramillo normal events. In this study, a reexamination of magnetostratigraphy and calcareous nannofossil biostratigraphy of this formation was carried out. The results show that the strata with stable remanent magnetizations have reversed magnetic polarities only, and the layers with marine sedimentary facies consistently contain specimens of large *Gephyrocapsa*. These updated results suggest that the Tananwan Formation was deposited within the interval of 1.46 - 1.24 Ma, corresponding to a short period of reversed magnetic polarity of the Matuyama Epoch.

Key words: Tananwan Formation, Magnetostratigraphy, Nannofossil, Siderite

Citation: Horng, C. S., 2014: Age of the Tananwan Formation in northern Taiwan: A reexamination of the magnetostratigraphy and calcareous nannofossil biostratigraphy. *Terr. Atmos. Ocean. Sci.*, 25, 137-147, doi: 10.3319/TAO.2013.11.05.01(TT)

---

## 1. INTRODUCTION

The Tananwan Formation, exposed on the Linkou Tableland in northwestern Taiwan, is characterized by its flat-lying strata consisting of loosely cohered sandstones and mudstones intercalated with conglomerates (Figs. 1a and 2a, c, d). Sedimentary facies analysis indicates that these sediments were deposited in nearshore environments with shallow water marine, beach, lagoon, tidal, delta, lacustrine, fluvial and alluvial lithofacies (Chen and Teng 1990; Chuang et al. 2012). Overlying the Tananwan Formation is the Linkou Formation composed of thick or massive conglomerates. This lithofacies change was due to uplifting episodes of northern Taiwan during the Plio-Pleistocene Penglai Orogeny.

To reconstruct the tectonic history of the Penglai Orogeny, it is important to understand the chronology of uplifting events. Over the past two decades, methods including electron spin resonance, pollen, magnetostratigraphy and calcareous nannofossil have been used to construct a more detailed chronology of the Tananwan Formation. These studies claimed that the succession strata of the Tananwan Formation may represent a long period in the Matuyama Epoch most likely covering the Olduvai and Jaramillo normal events (Lee et al.

2002), or a short time interval between 0.9 and 0.7 Ma (Shih 1991; Tseng et al. 1992; Wei et al. 2009).

Regardless of this difference in the estimated age, ambiguous interpretations and conflicting observations exist among these studies. For the magnetostratigraphy, Lee et al. (2002) reported that most of the sites they surveyed in the Tananwan Formation had reversed magnetic polarity records, but some had abnormal paleomagnetic directions that were interpreted equivocally to be the Olduvai and Jaramillo normal polarity events in the Matuyama Epoch or to be disturbed by coarse sediments deposited in high-energy environments. These two interpretations contradict each other because the former one suggests a low sedimentation rate for the Tananwan Formation (i.e., 0.1 mm yr<sup>-1</sup>, derived from a 80-m succession of strata with a time duration of about 0.8 million years, see Fig. 4 of Lee et al. 2002), whereas the latter one implies a dynamic setting with high and variable sedimentation rates.

Tseng et al. (1992) studied the calcareous nannofossil biostratigraphy of the Tananwan Formation and reported the presence of large *Gephyrocapsa*. According to Rio (1982) and Rio et al. (1990), the genus *Gephyrocapsa* Kamptner underwent morphologic evolution during the late Pliocene-Pleistocene. This genus can be divided into four categories

---

\* Corresponding author  
E-mail: cshorng@earth.sinica.edu.tw

based on biometric definition: (1) small *Gephyrocapsa* (lumping all forms with sizes  $< 3.5 \mu\text{m}$ ), (2) medium *Gephyrocapsa* ( $4 - 5.5 \mu\text{m}$ ), (3) large *Gephyrocapsa* ( $> 5.5 \mu\text{m}$ ), and (4) *Gephyrocapsa* sp. 3 ( $> 4 \mu\text{m}$ , characterized by a bridge nearly parallel to the short axis of placolith). These four categories are useful for identifying subdivisions of the biostratigraphy based on their occurrence datum events whose ages have been dated and are shown in Fig. 2b (Rio 1982; Rio et al. 1984; Wei 1993; Berggren et al. 1995; Raffi et al. 2006). Despite Tseng et al. (1992) consistently finding specimens of large *Gephyrocapsa* in the Tananwan Formation, they did not assign an age of 1.46 - 1.24 Ma (see Fig. 2b) to the formation. Instead, they proposed that the Tananwan Formation is younger than 0.9 Ma according to their own pollen stratigraphy. In contrast, Wei et al. (2009) regarded the specimens of *Gephyrocapsa* in the Tananwan Formation as having sizes less than  $5.5 \mu\text{m}$  and morphologic features of *Gephyrocapsa* sp. 3. Together with other

evidence such as the absence of *Reticulofenestra asanoi*, Wei et al. (2009) concluded that the age of Tananwan Formation is confined to 0.89 - 0.78 Ma. In an attempt to clarify whether the Olduvai and Jaramillo normal events suggested by Lee et al. (2002) are reasonable and to reconcile the differences regarding the sizes of *Gephyrocapsa* identified by Tseng et al. (1992) and Wei et al. (2009), a reexamination of magnetostratigraphy and calcareous nannofossil biostratigraphy of the Tananwan Formation is needed.

## 2. MATERIALS AND METHODS

Samples for paleomagnetic and nannofossil studies were collected along rivers or roads where outcrops of the Tananwan Formation are accessible (Fig. 1a). A total of 19 sites covering the entire Tananwan sequence were obtained from stratigraphic heights ranging from *ca.* 20 to 150 m (Fig. 2a). At each site, 5 - 6 cores (25 mm in diameter) were

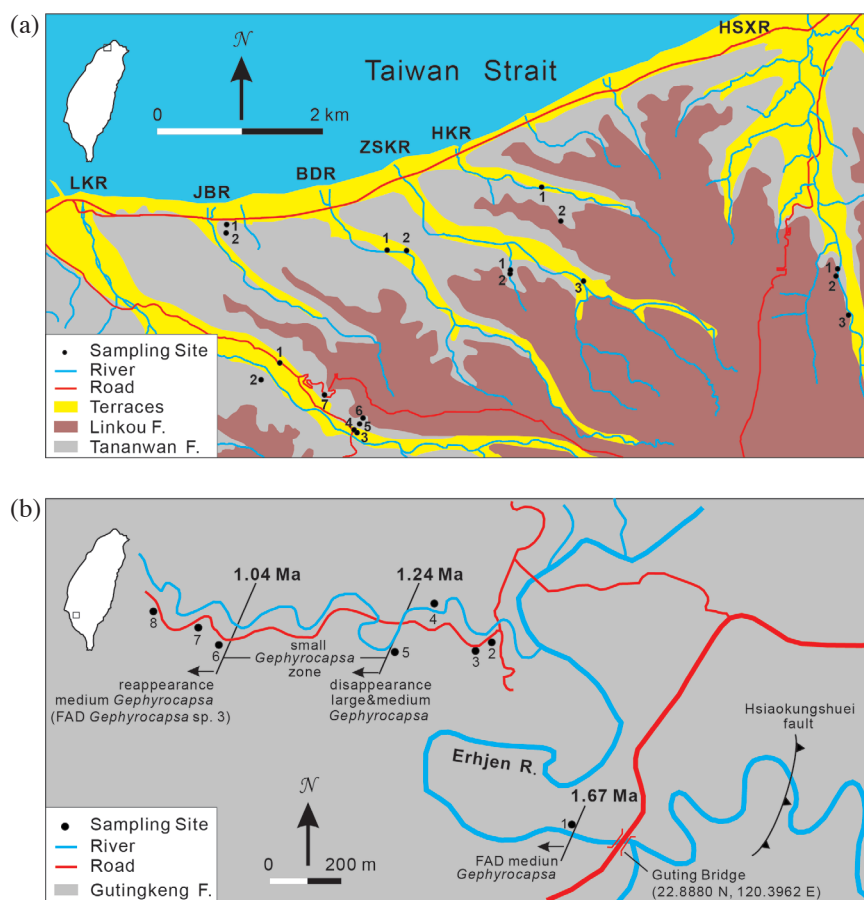


Fig. 1. (a) Map showing locations of 19 sampling sites in the Tananwan Formation on the Linkou Tableland in northwestern Taiwan. Samples were collected along rivers or roads. LKR, JBR, BDR, ZSKR, HKR, HSXR represent Linkou, Jiabao, Baodou, Zueishukeng, Houkeng, and Hongshuixian Rivers, respectively. (b) Map showing locations of 8 sampling sites in the Gutingkeng Formation of the Erhjen River (EJR) section in southwestern Taiwan. Ages of the strata are younger westwards with three well-dated calcareous nannofossil datum events indicated [1.67 Ma: the first appearance datum (FAD) of medium *Gephyrocapsa*; 1.24 Ma: the disappearance of large and medium *Gephyrocapsa*; 1.04 Ma: the reappearance of medium *Gephyrocapsa* or FAD of *Gephyrocapsa* sp. 3; Chen et al. 1977; Shea and Horng 1999; Raffi et al. 2006; Horng and Shea 2007]. During the time interval of 1.24 - 1.04 Ma, medium and large *Gephyrocapsa* disappeared, and only small *Gephyrocapsa* survived. Thus, this interval is called the small *Gephyrocapsa* zone.

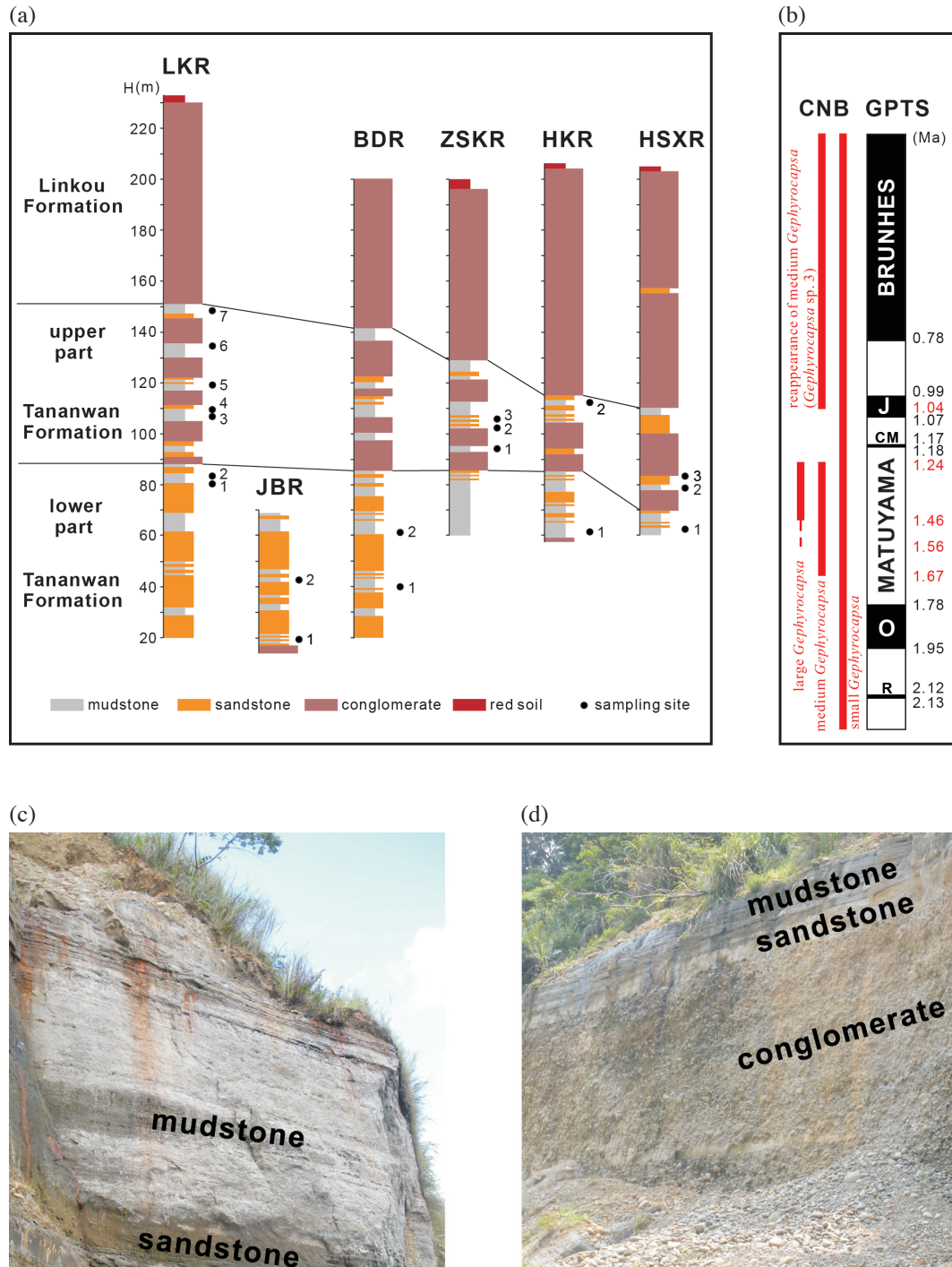


Fig. 2. (a) Stratigraphic profiles showing the Tanawan and the Linkou Formations and their lithological variations along six river (LKR, JBR, BDR, ZSKR, HKR, and HSXR) sections on the Linkou Tableland in northwestern Taiwan (after Chuang et al. 2012). The stratigraphic heights (H) of sampling sites on each section are indicated. (b) Geomagnetic polarity time scale (GPTS) and calcareous nannofossil biostratigraphy (CNB) of genus *Gephyrocapsa* since 2.2 Ma. Ages of *Gephyrocapsa* morphologic evolutionary events are 1.67 Ma for the FAD of medium *Gephyrocapsa*, 1.56 Ma for the FAD of large *Gephyrocapsa*, 1.46 Ma for the onset of consistent occurrence of large *Gephyrocapsa*, 1.24 Ma for the disappearance of medium and large *Gephyrocapsa*, and 1.04 Ma for the reappearance of medium *Gephyrocapsa* (or the FAD of *Gephyrocapsa* sp. 3). Normal polarity events within the Matuyama reversed Epoch are Reunion (R), Olduvai (O), Cobb Mountain (CM), and Jaramillo (J) (Horng et al. 2002; Lourens et al. 2004; Raffi et al. 2006). (c - f) Field photos showing characteristics of the Tanawan Formation: (c) flat-lying sandstone and mudstone layers; (d) intercalation of conglomerate in mudstone and sandstone strata; (e - f) colors of siderite-bearing strata changed from dark gray to yellow or reddish brown depending on weathering extents.

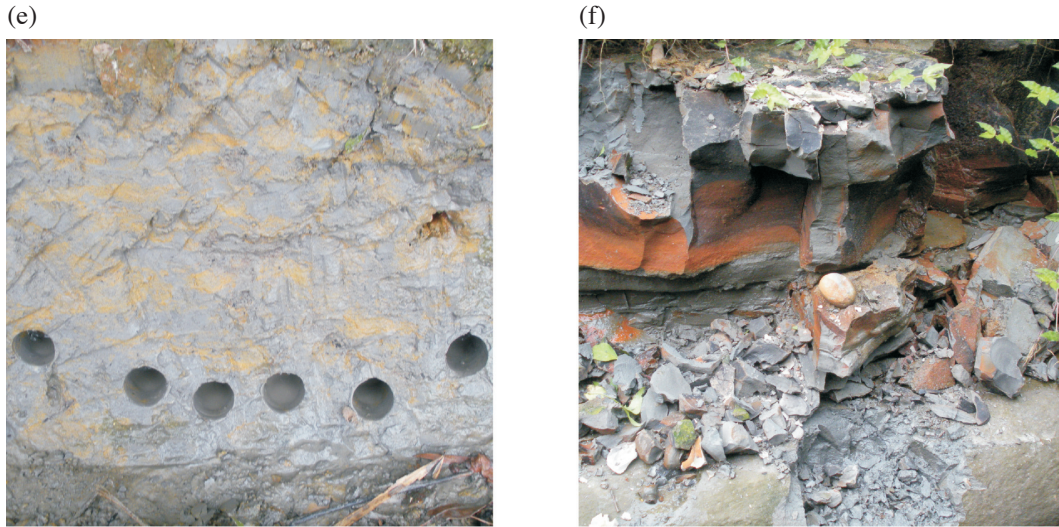


Fig. 2. (Continued)

drilled after removing weathered surface of outcrops. Cores were oriented (azimuth and dip) with a mechanical device mounted with a magnetic compass. Non-oriented samples were also taken from the sites for studying magnetic mineralogy and calcareous nannofossil biostratigraphy. Because the morphologic evolutionary events of *Gephyrocapsa* are well preserved in the Gutingkeng Formation of the Erhjen River (EJR) section in southwestern Taiwan (Chen et al. 1977; Shea and Horng 1999; Horng and Shea 2007), samples from the EJR section straddling the stratigraphic levels from the first appearance datum (FAD) of medium *Gephyrocapsa* up to the post-FAD of *Gephyrocapsa* sp. 3 (Fig. 1b) were also collected for comparison with calcareous nannofossils in the Tananwan Formation.

In the laboratory, specimens (22 mm in length) were cut from oriented cores and then subjected to paleomagnetic analysis. For the natural remanent magnetization (NRM), specimens were measured with a 2G Enterprises superconducting rock magnetometer to obtain their intensities (J), declinations (Dec) and inclinations (Inc). Thermal demagnetization was then carried out by a Magnetic Measurements Ltd. thermal demagnetizer that has a low-field cooling chamber. Sixteen heating steps from room temperature up to 680°C were used (i.e., 25, 120, 160, 200, 240, 280, 320, 360, 400, 440, 480, 520, 560, 600, 640, and 680°C) to obtain stable characteristic remanent magnetization (ChRM) after erasing viscous and unstable secondary magnetizations. To monitor possible changes in magnetic minerals and magnetic properties during heating, low-field magnetic susceptibility ( $\chi$ ) was measured on specimens after each heating step with a Bartington Instruments MS2B magnetic susceptibility system. To characterize magnetic mineralogy in specimens and to interpret the behavior of remanent magnetizations during thermal demagnetization, magnetic separation from non-ori-

ented samples using a rare earth magnet housed in a plastic sheath was used.

Low-temperature magnetic measurements and X-ray diffraction (XRD) analysis were carried out on magnetic extracts using a Quantum Design SQUID vibrating sample magnetometer (VSM) and a Rigaku Miniflex table top unit (Cu-K $\alpha$  radiation), respectively. For the low-temperature magnetic measurements, magnetic extracts were cooled from room temperature to 5 K in zero field in the SQUID VSM. At 5 K, a 5 T DC field was applied and then switched off to impart a low-temperature saturation isothermal remanent magnetization (SIRM). SIRM curves were measured during warming in zero field up to 300 K at a warming rate of 3 K min<sup>-1</sup> to detect magnetic transitions revealed from magnetic extracts. Then X-ray scans were run from 4 to 80° (2 $\theta$ ) to verify magnetic mineralogy suggested by SQUID VSM measurements. The results are presented after subtraction of the background.

Smear slides for nannofossil identification were prepared from small chips of non-oriented samples and then examined under an optical microscope and a scanning electron microscope (SEM). Observations were particularly focused on *Gephyrocapsa* spp. and their sizes were determined based on SEM images.

### 3. RESULTS AND DISCUSSION

#### 3.1 Magnetic Mineralogy

Low-temperature magnetic measurements of magnetic extracts from the Tananwan Formation show that three magnetic transitions occur near 20, 40, and 115 K upon warming of SIRM curves (Figs. 3a - b). The transition at ~115 K is the Verwey transition that is a diagnostic feature of magnetite (Fe<sub>3</sub>O<sub>4</sub>) at low temperatures (Verwey 1939; Özdemir

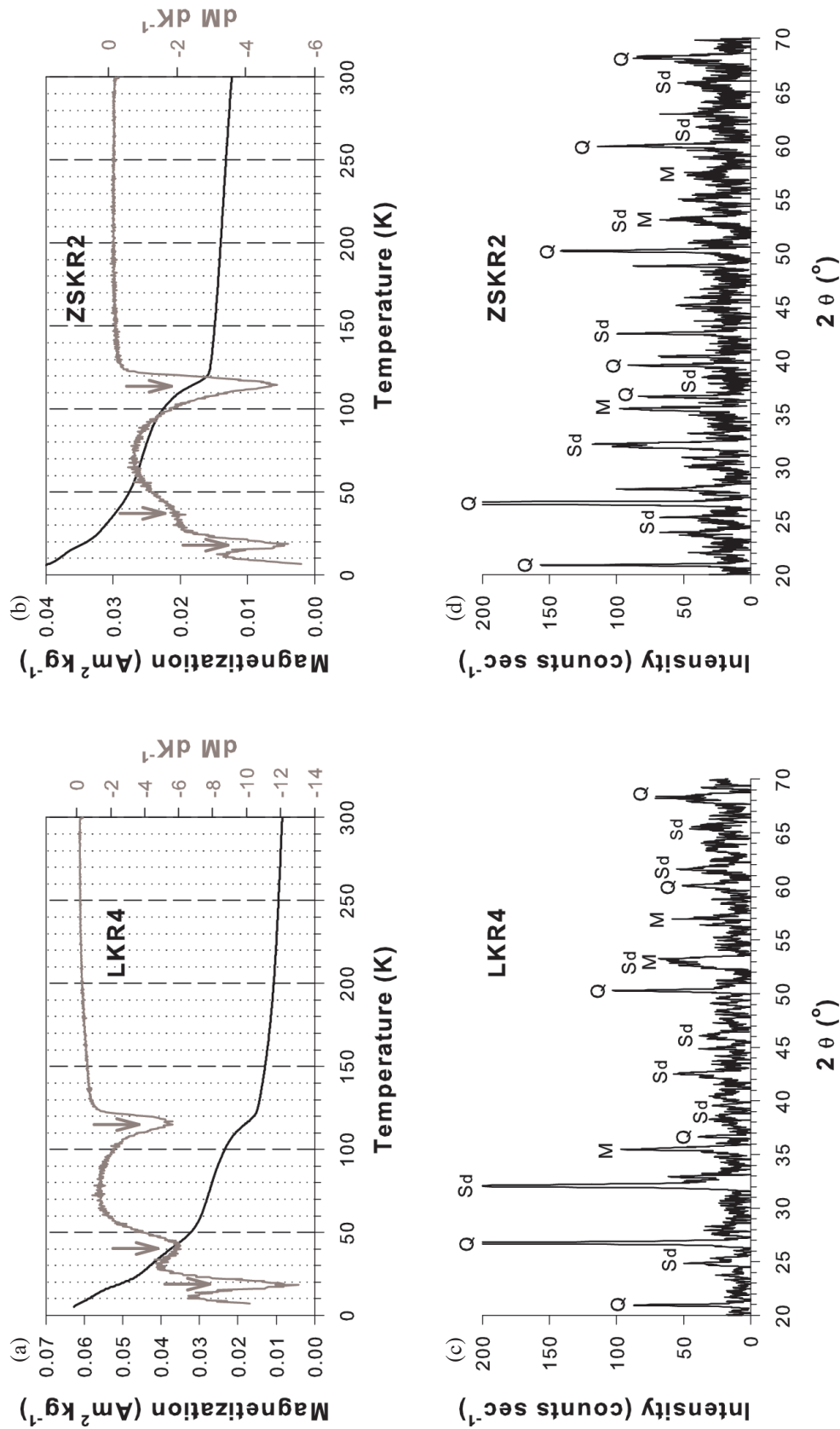


Fig. 3. (a - b) Low-temperature analysis of SIRM (5 T) acquired at 5 K for magnetic extracts from Sites LKR4 and ZSKR2 of the Tanawan Formation, with measurements made during zero-field warming from 5 to 300 K. The derivative of the SIRM (dM dK<sup>-1</sup>) is labeled on the y-coordinate at the right-hand axis to indicate magnetic transitions at ca. 20, 40, and 115 K. (c - d) X-ray diffractograms of the same magnetic extracts showing characteristic peaks of magnetite (M), siderite (Sd), and quartz (Q).

et al. 1993). For the transition at ~40 K, siderite ( $\text{FeCO}_3$ ), pyrrhotite ( $\text{Fe}_7\text{S}_8$ ) and rhodochrosite ( $\text{MnCO}_3$ ) are three possible minerals causing the transition (Dekkers et al. 1989; Rochette et al. 1990; Housen et al. 1996). For the transition at ~20 K, however, no mineral responsible for it has been reported in literature, which is worthwhile to investigate in the future. XRD analysis on the magnetic extracts further confirms that magnetite and siderite are commonly present in the Tananwan Formation (Figs. 3c - d). Because siderite may form either in marine or in fresh-water environments (Mozley 1989; Pye et al. 1990), it is suggested that siderite in the Tananwan Formation was formed through diagenetic processes. Field observations show that siderite-bearing strata are susceptible to weathering. The oxidation of siderite to ferric iron minerals usually results in changes in rock color from dark gray to yellow or even reddish brown, depending on the extents of weathering (Figs. 2e - f).

### 3.2 Magnetostratigraphy

NRM intensity ( $J_0$ ) and low-field magnetic susceptibil-

ity ( $\chi_0$ ) of Tananwan specimens before thermal demagnetization (i.e., at 25°C) fall in the range of 2.8 -  $155 \times 10^{-3} \text{ Am}^2$  and 8.9 -  $36.1 \times 10^{-6}$ , respectively (Table 1). The wide range of these values implies large variations in magnetic compositions and/or concentrations. The thermal demagnetization results from this study can be classified into two types, designated as Type S (stable) and Type U (unstable). The examples shown in Fig. 4 illustrate the behavior of the two types during thermal demagnetization treatments. In general, each Type S specimen has a rather stable remanence below ~360°C and may slightly or dramatically change its remanent directions at higher temperatures (Figs. 4a - h). It is evident from Figs. 4a - h that only reversed magnetic polarities were deciphered in Type S specimens according to their stable ChRMs (see Table 1). In contrast, Type U samples always show scattering and unstable remanences during thermal demagnetization. Among Type U, a few samples may have slightly scattering directions and still display a reversed magnetic polarity record (e.g., Fig. 4i), but most of Type U samples are too unstable to decipher their magnetic polarities (Figs. 4j - l and Table 1).

Table 1. Characteristics of 19 sampling sites in the Tananwan Formation along 6 river sections (see Fig. 1a) and paleomagnetic properties revealed during thermal demagnetization treatments of the specimens.

Site	Lat. (°N)	Long. (°E)	H (m)	Specimen	$J_0$ ( $10^{-3} \text{ Am}^2$ )	$\chi_0$ ( $10^{-6}$ )	Dec (°)	Inc (°)	Temp (°C)	Magnetic Polarity
LKR1	25.1053	121.3262	81	2A	8.2	19.4	175.7	-25.4	160-360	reversed
LKR2	25.1033	121.3239	83	1A	92.7	20.9	182.1	-32.1	25-640	reversed
LKR3 <sup>#</sup>	25.0976	121.3355	108	4A	67.2	23.9	196.5	-39.8	25-360	reversed
LKR4 <sup>#</sup>	25.0977	121.3353	109	4A	143.0	28.5	195.4	-42.1	120-640	reversed
LKR5	25.0984	121.3360	119	4A	22.8	24.7	171.2	-36.3	25-360	reversed
LKR6	25.0991	121.3363	135	3A	5.9	18.9	204.7	-9.1	440-560	reversed
LKR7	25.1016	121.3317	147	1A	4.6	8.9	N/A	N/A	N/A	N/A
JBR1	25.1206	121.3198	18	1A	9.5	17.3	N/A	N/A	N/A	N/A
JBR2	25.1197	121.3197	42	4A	26.8	22.8	175.2	-50.8	160-400	reversed
BDR1	25.1177	121.3394	40	3A	10.6	23.1	188.9	-46.6	25-240	reversed
BDR2 <sup>#</sup>	25.1175	121.3419	61	5A	155.0	36.1	195.1	-51.2	25-400	reversed
ZSKR1	25.1155	121.3542	95	1A	33.0	21.7	160.2	-32.9	25-400	reversed
ZSKR2	25.1152	121.3541	103	4A	116.0	28.6	178.7	-47.0	120-360	reversed
ZSKR3	25.1142	121.3633	105	2A	22.4	20.2	205.7	-46.6	25-400	reversed
HKR1 <sup>#</sup>	25.1247	121.3583	62	3A	48.5	19.4	181.9	-28.8	120-360	reversed
HKR2	25.1209	121.3606	115	1A	2.8	16.6	N/A	N/A	N/A	N/A
HSXR1 <sup>#</sup>	25.1155	121.3944	64	1A	82.5	22.0	188.7	-33.9	25-400	Reversed
HSXR2	25.1146	121.3942	78	3A	73.8	26.7	184.4	-41.5	120-360	Reversed
HSXR3	25.1104	121.3957	84	4A	3.6	18.1	N/A	N/A	N/A	N/A

Note: #: sites containing nannofossils; Lat. & Long.: latitude and longitude; H: height.

$J_0$  and  $\chi_0$ : intensity of NRM and low-field magnetic susceptibility at 25°C.

Dec and Inc: declination and inclination of stable ChRM.

Temp: temperature range showing stable ChRM; N/A: not available.

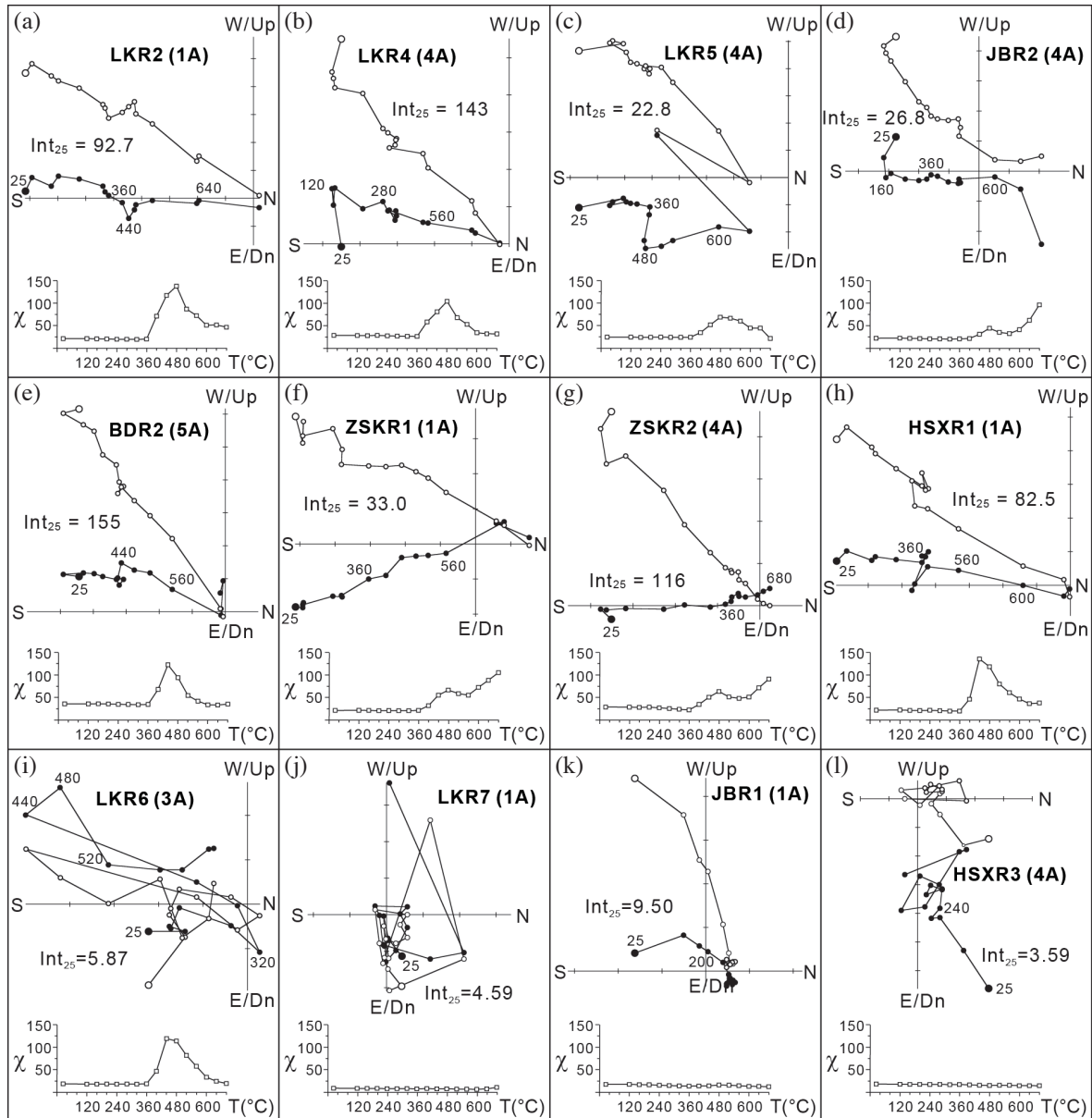


Fig. 4. Representative thermal demagnetization diagrams of specimens from various sites in the Tanawan Formation. Because of the flat-lying strata, no bedding correction was made on the specimens. Solid circles: horizontal projections (declinations); open circles: vertical projections (inclinations). Values next to the solid circles are temperatures. Intensity of NRM at 25°C ( $Int_{25}$ ,  $10^{-3} \text{ Am}^2$ ) of each specimen is indicated. Below each diagram is a plot of low-field magnetic susceptibility ( $\chi$ ,  $10^{-6}$ ) versus temperature. (a - h) Type S specimens with stable reversed ChRMs. (i - l) Type U specimens showing unstable remanent magnetizations.

Changes in magnetic susceptibility during thermal demagnetization are also shown in Fig. 4. Samples with reversed magnetic polarity records, as illustrated in Figs. 4a - i, undergo remarkable changes in susceptibility at temperatures above 360°C, whereas samples showing non-resolvable polarity records (Figs. 4j - l) not only have low  $\chi_0$  (see Table 1) but also little change in  $\chi$  during heating. The changes in  $\chi$  above 360°C shown in Figs. 4a - i imply that the transformation from ferrous to ferric iron minerals has occurred during thermal demagnetization. Siderite is commonly present in the Tanawan Formation (Fig. 3) and can transform into other forms

of magnetic minerals (i.e., secondary magnetite, maghemite, and hematite) during heating (Pan et al. 2000). Changes in susceptibility occurring above 360°C can be mainly caused by high-temperature oxidation of siderite. Because siderite is susceptible to weathering or oxidation, the presence of siderite in rocks also means that these rocks or samples are fresh and the primary depositional magnetite shown in Fig. 3 is still well-preserved. Therefore, the reversed magnetic polarities recorded in the siderite-bearing samples (Figs. 4a - i) are reliable. On the other hand, samples with low magnetic susceptibility (Figs. 4j - l and Table 1) must have experienced

weathering to a large extent (see Figs. 2e - f), rendering their magnetic remanences unstable and polarities unclear.

### 3.3 Calcareous Nannofossil Biostratigraphy

Because of various depositional facies in nearshore environments, the strata in the Tananwan Formation com-

monly or poorly may contain fossils. In this study, five sites (i.e., LKR3, LKR4, BDR2, HKR1, and HSXR1) with marine facies yield calcareous nannofossils with rather good preservation (Figs. 1a and 2a). *Gephyrocapsa* spp. and *Pseudomilania lacunosa* are the dominant indigenous species in the nannofossil assemblage. Shown in micrographs 1 - 28 of Fig. 5 are the representative *Gephyrocapsa* spp. with sizes

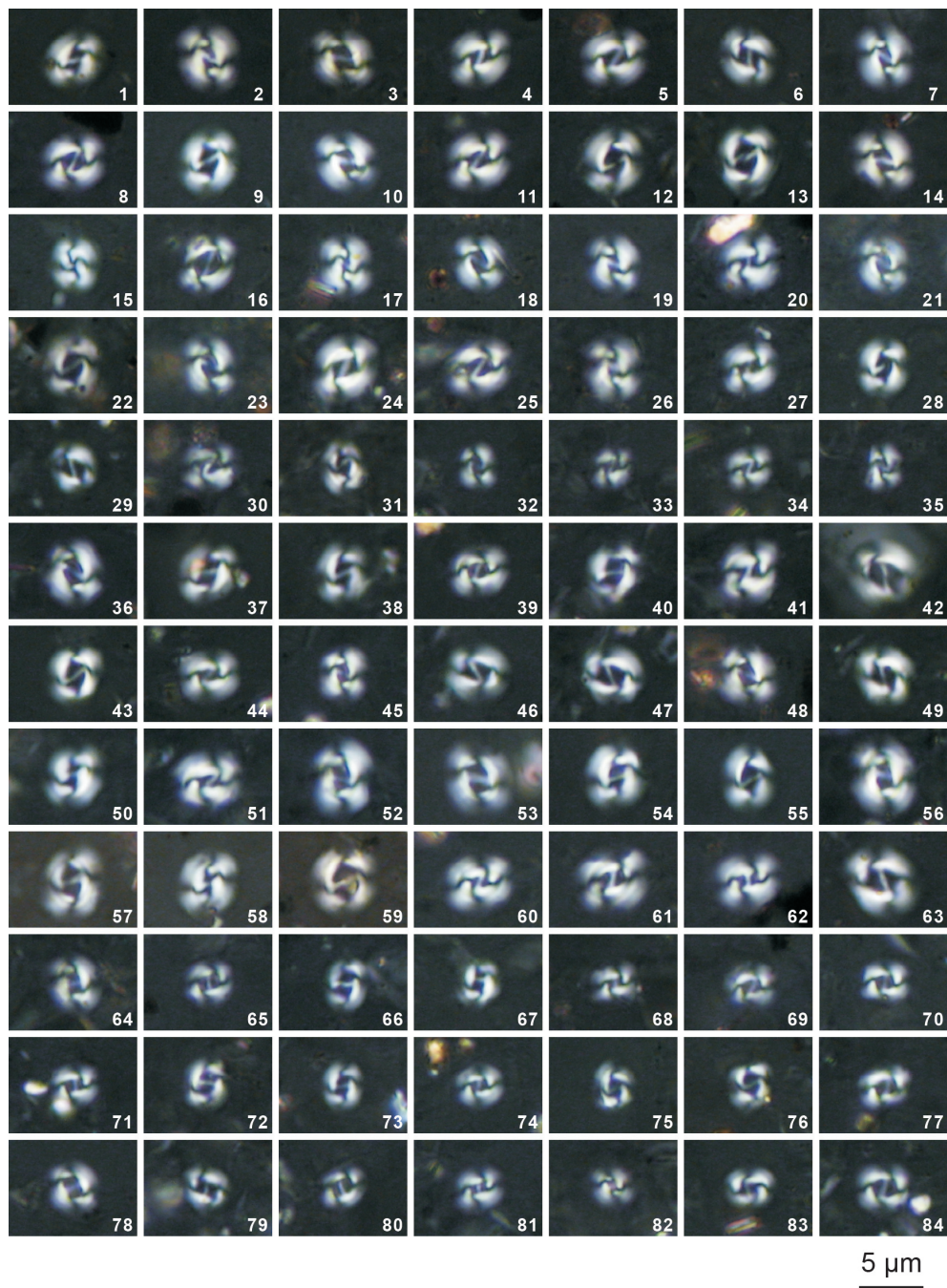


Fig. 5. Optical micrographs of *Gephyrocapsa* with sizes larger than 4  $\mu\text{m}$  from 5 sites (LKR3, LKR4, BDR2, HKR1, and HSXR1) in the Tananwan Formation and 8 sites (EJR1 - EJR8) in the Gutingkeng Formation. All graphs are shown at the same scale (scale bar = 5  $\mu\text{m}$ ). (1 - 7) LKR3; (8 - 14) LKR4; (15 - 21) BDR2; (22 - 23) HKR1; (24 - 28) HSXR1; (29 - 35) EJR1 (the FAD of medium *Gephyrocapsa*, at 1.67 Ma); (36 - 42) EJR2; (43 - 49) EJR3; (50 - 56) EJR4; (57 - 63) EJR5 (near the disappearance datum of medium and large *Gephyrocapsa*, at  $\sim$ 1.24 Ma); (64 - 70) EJR6 (the reappearance datum of medium *Gephyrocapsa* or FAD of *Gephyrocapsa* sp. 3, at 1.04 Ma); (71 - 77) EJR7; (78 - 84) EJR8.

larger than 4  $\mu\text{m}$ . Micrographs 29 - 84 in Fig. 5 illustrate the morphologic evolution of *Gephyrocapsa*, showing the size variations of this genus at 8 sites in the Gutingkeng Formation along the EJR section (Fig. 1b) covering stratigraphic levels from the FAD of medium *Gephyrocapsa* (at 1.67 Ma), through the disappearance datum of large and medium *Gephyrocapsa* (at 1.24 Ma), and up to the post-FAD of *Gephyrocapsa* sp. 3 (i.e., younger than the reappearance datum of medium *Gephyrocapsa*, < 1.04 Ma) (Fig. 2b). It is clear from Fig. 5 that the sizes of *Gephyrocapsa* spp. in the Tanawan Formation (micrographs 1 - 28) are almost equivalent to those (micrographs 36 - 63 in Fig. 5) of the four sites (i.e., EJR2 - EJR5) in the Gutingkeng Formation. SEM images of *Gephyrocapsa* spp. from Sites LKR3 and EJR5 further reveal that some *Gephyrocapsa* specimens have sizes over 5.5  $\mu\text{m}$  (e.g., micrographs 1 - 3 and 13 - 14 in Fig. 6), indicating that large *Gephyrocapsa* spp. are present both in the Tanawan and Gutingkeng Formations. According to the consistent occurrence of large *Gephyrocapsa*, the age of the Tanawan Formation is estimated to be within 1.46 - 1.24 Ma, corresponding to a short, magnetically reversed interval in the Matuyama Epoch (Fig. 2b). The paleomagnetic results

described here where only reversed magnetic polarities are preserved in the Tanawan Formation (Table 1) support this interpretation.

It should be noted that large and medium *Gephyrocapsa* in the Tanawan and Gutingkeng Formations with ages older than 1.24 Ma are characterized by a bridge that aligns diagonally to the short axis of placolith with either a wide open or a closed central area (micrographs 1 - 16 in Fig. 6). These characteristics can be also recognized with optical microscopy (micrographs 1 - 63 in Fig. 5). However, another type of medium *Gephyrocapsa* (i.e., *Gephyrocapsa* sp. 3) that occurs only after 1.04 Ma has a bridge nearly parallel to the short axis of placolith, as shown in the 3 younger sites of the Gutingkeng Formation (i.e., EJR6 - EJR8; see micrographs 64 - 68, 71 - 72, 78 - 82 in Fig. 5 and micrographs 17 - 20 in Fig. 6). In other words, the results of this study do not support the interpretation in Wei et al. (2009) that *Gephyrocapsa* sp. 3 is present in the Tanawan Formation.

#### 4. CONCLUSIONS

From a reexamination of the nannofossil biostratigraphy

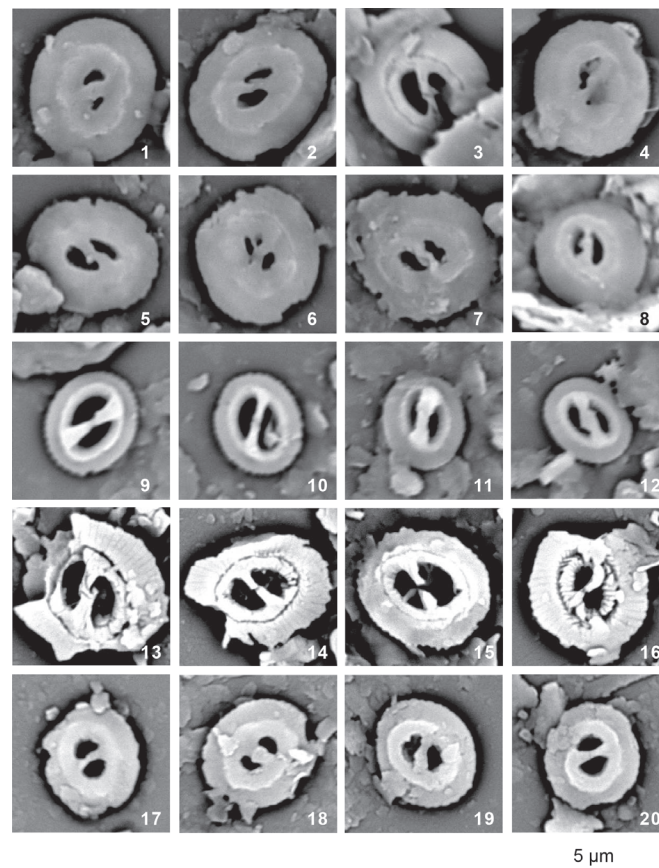


Fig. 6. Scanning electron micrographs of *Gephyrocapsa* with sizes larger than 4  $\mu\text{m}$  from Site LKR3 in the Tanawan Formation and Sites EJR5 and EJR6 in the Gutingkeng Formation. All graphs are shown at the same scale (scale bar = 5  $\mu\text{m}$ ). (1 - 12) LKR3; (13 - 16) EJR5 (at ~1.24 Ma); (17 - 20) EJR6 (at 1.04 Ma). It is noted that the alignment of bridge of *Gephyrocapsa* shown in micrographs 17 - 20 is nearly parallel to the short axis of placolith (i.e., *Gephyrocapsa* sp. 3), while the alignment of others is diagonal.

of the Tananwan Formation, it is suggested that the age of this formation should fall within the interval of 1.46 - 1.24 Ma, which is older than the 0.9 - 0.7 Ma interval proposed by previous investigations (Shih 1991; Tseng et al. 1992; Wei et al. 2009). The time interval at 1.46 - 1.24 Ma suggests that the Tananwan Formation should record reversed magnetic polarities only. A revisit of the magnetostratigraphy lends support to the revision and rules out the existence in the formation of two normal polarity events (i.e., Jaramillo and Olduvai) proposed by Lee et al. (2002). This study also demonstrates that authigenic siderite is commonly present in this formation. Thus, interpretation of paleomagnetic data for the Tananwan Formation should be made with caution because siderite-bearing rocks may undergo more or less weathering and their rock magnetic properties will change accordingly.

**Acknowledgements** The author is grateful to Chao-Ming Chuang for field assistance and to Kuo-Hang Chen, Chun-Hung Lin and Chung-Yi Tseng for their help both in the field and the lab. Thanks are also due to Chih-An Huh for revising the first draft and to Wen-Rong Chi and Kai-Shuan Shea for reviewing the manuscript. This work is supported by the Institute of Earth Sciences, Academia Sinica and National Science Council grant NSC96-2116-M-001-013-MY2.

## REFERERENCES

- Berggren, W. A., F. J. Hilgen, C. G. Langereis, D. V. Kent, J. D. Obradovich, I. Raffi, M. E. Raymo, and N. J. Shackleton, 1995: Late Neogene chronology: New perspectives in high-resolution stratigraphy. *Geol. Soc. Am. Bull.*, **107**, 1272-1287, doi: 10.1130/0016-7606(1995)107<1272:LNCNPI>2.3.CO;2. [[Link](#)]
- Chen, P. H., C. Y. Huang, T. C. Huang, and L. P. Tsai, 1977: A study of the late Neogene marine sediments of the Chishan area, Taiwan: Paleomagnetic stratigraphy, biostratigraphy, and paleoclimate. *Mem. Geol. Soc. China*, **2**, 169-190.
- Chen, W. F. and L. S. Teng, 1990: Depositional environment of Quaternary deposits of the Linkou Tableland, north-western Taiwan. *Proc. Geol. Soc. China*, **33**, 39-63.
- Chuang, C. M., W. F. Chen, and L. S. Teng, 2012: Depositional facies and environment of Tananwan Formation, Linkou Tableland. *West. Pac. Earth Sci.*, **12**, 127-156.
- Dekkers, M. J., J. L. Mattéi, G. Fillion, and P. Rochette, 1989: Grain-size dependence of the magnetic behavior of pyrrhotite during its low-temperature transition at 34 K. *Geophys. Res. Lett.*, **16**, 855-858, doi: 10.1029/GL016i008p00855. [[Link](#)]
- Horng, C. S. and K. S. Shea, 2007: The Quaternary magnetobiostatigraphy of Taiwan and Penglai orogenic events. *Spec. Publ. Cent. Geol. Sur., MOEA*, **18**, 51-83.
- Horng, C. S., M. Y. Lee, H. Pälike, K. Y. Wei, W. T. Liang, Y. Iizuka, and M. Torii, 2002: Astronomically calibrated ages for geomagnetic reversals within the Matuyama chron. *Earth Planets Space*, **54**, 679-690.
- Housen, B. A., S. K. Banerjee, and B. M. Moskowitz, 1996: Low-temperature magnetic properties of siderite and magnetite in marine sediments. *Geophys. Res. Lett.*, **23**, 2843-2846, doi: 10.1029/96GL01197. [[Link](#)]
- Lee, T. Q., Y. T. Lue, W. R. Chi, and L. S. Teng, 2002: Paleomagnetic study of the Kuanyinshan and Tanawan Formations, northern Taiwan. *West. Pac. Earth Sci.*, **2**, 27-36.
- Lourens, L., F. Hilgen., N. J. Shackleton, J. Laskar, and D. Wilson, 2004: The Neogene Period. In: Gradstein, F. M., J. G. Ogg, and A. G. Smith (Eds.), *A Geological Time Scale 2004*, Cambridge University Press, Cambridge, 409-440.
- Mozley, P. S., 1989: Relation between depositional environment and the elemental composition of early diagenetic siderite. *Geology*, **17**, 704-706, doi: 10.1130/0091-7613(1989)017<0704:RBDEAT>2.3.CO;2. [[Link](#)]
- Özdemir, Ö., D. J. Dunlop, and B. M. Moskowitz, 1993: The effect of oxidation on the Verwey transition in magnetite. *Geophys. Res. Lett.*, **20**, 1671-1674, doi: 10.1029/93GL01483. [[Link](#)]
- Pan, Y., R. Zhu, S. K. Banerjee, J. Gill, and Q. Williams, 2000: Rock magnetic properties related to thermal treatment of siderite: Behavior and interpretation. *J. Geophys. Res.*, **105**, 783-794, doi: 10.1029/1999JB900358. [[Link](#)]
- Pye, K., J. A. D. Dickson, N. Schiavon, M. L. Coleman, and M. Cox, 1990: Formation of siderite-Mg-calcite-iron sulphide concretions in intertidal marsh and sandflat sediments, north Norfolk, England. *Sedimentology*, **37**, 325-343, doi: 10.1111/j.1365-3091.1990.tb00962.x. [[Link](#)]
- Raffi, I., J. Backman, E. Fornaciari, H. Pälike, D. Rio, L. Lourens, and F. Hilgen, 2006: A review of calcareous nannofossil astrobiochronology encompassing the past 25 million years. *Quat. Sci. Rev.*, **25**, 3113-3137, doi: 10.1016/j.quascirev.2006.07.007. [[Link](#)]
- Rio, D., 1982: The fossil distribution of coccolithophore genus *Gephyrocapsa* Kamptner and related Pliocene-Pleistocene chronostratigraphic problems. *Init. Repts. DSDP*, **68**, 325-343, doi: 10.2973/dsdp.proc.68.109.1982. [[Link](#)]
- Rio D., R. Sprovieri, and I. Raffi, 1984: Calcareous plankton biostratigraphy and biochronology of the Pliocene-Lower Pleistocene succession of the Capo Rossello area, Sicily. *Mar. Micropaleontol.*, **9**, 135-180, doi: 10.1016/0377-8398(84)90008-2. [[Link](#)]
- Rio, D., I. Raffi, and G. Villa, 1990: Pliocene-Pleistocene calcareous nannofossil distribution patterns in the western Mediterranean. *Proc. ODP. Sci. Results*, **107**, 513-533, doi: 10.2973/odp.proc.sr.107.164.1990. [[Link](#)]

- Rochette, P., G. Fillion, J. L. Mattéi, and M. J. Dekkers, 1990: Magnetic transition at 30-34 K in Fe<sub>7</sub>S<sub>8</sub>: Insight into a widespread occurrence of pyrrhotite in rocks. *Earth Planet. Sci. Lett.*, **98**, 319-328.
- Shea, K. S. and C. S. Horng, 1999: Recognition of the Pliocene-Pleistocene boundary based on *Pulleniatina* coiling change: A case study of the Erhjen-chi section, southwestern Taiwan. *Quat. Sci.*, **6**, 549-555.
- Shih, T. S., 1991: A study of ESR dating on mollusk fossils. Master Thesis, National Taiwan University, Taiwan, 168 pp.
- Tseng, M. H., P. M. Liew, W. R. Chi, and T. S. Shih, 1992: Pollen analysis of the Tanawan Formation, Northern Taiwan. *J. Geol. Soc. China*, **35**, 247-259.
- Verwey, E. J. W., 1939: Electronic conduction of magnetite (Fe<sub>3</sub>O<sub>4</sub>) and its transition point at low temperatures. *Nature*, **144**, 327-328, doi: 10.1038/144327b0. [[Link](#)]
- Wei, K. Y., C. K. Zhuang, and C. M. Zhuang, 2009: Biochronology study of the Tanawan Formation: A revisit. *Spec. Publ. Cent. Geol. Surv., MOEA*, **22**, 149-164.
- Wei, W., 1993: Calibration of upper Pliocene-lower Pleistocene nannofossil events with oxygen isotope stratigraphy. *Paleoceanography*, **8**, 85-99, doi: 10.1029/92PA02504. [[Link](#)]